Mobility of the N-Terminal Segment of Rabbit Skeletal Muscle F-Actin Detected by ^{1}H and ^{19}F Nuclear Magnetic Resonance Spectroscopy

Daniela Heintz, Harry Kany, and Hans Robert Kalbitzer*

Department of Biophysics, Max Planck Institute for Medical Research, Jahnstrasse 29, D-69120 Heidelberg, Germany

Received May 15, 1996; Revised Manuscript Received July 1, 1996[⊗]

ABSTRACT: After polymerization filamentous actin (F-actin) still shows a number of rather narrow ^{1}H NMR signals in its Mg^{2+} form which are quenched when Mg^{2+} is replaced by Ca^{2+}. These resonances originate from mobile residues in F-actin. For assignment of these resonances three different strategies were used, the fluorine labeling of Cys-374 by 4-(perfluoro-*tert*-butyl)phenyliodoacetamide, binding studies with antibodies (Fab) against the seven N-terminal amino acids of actin, and two-dimensional ^{1}H NMR spectroscopy of a highly concentrated F-actin sample. In contrast to the effects detected earlier by ^{1}H NMR spectroscopy, ^{19}F NMR spectroscopy of actin labeled at its C-terminal cysteine shows no significant spectral changes in dependence on the divalent ion present. In its G- (globular) form a strong, narrow ^{19}F resonance can be observed at 15.06 ppm (relative to the external standard trifluoroacetic acid) which is broadened substantially after polymerization of actin. At 283 K the corresponding transverse relaxation time T_2 decreases from 16.7 ms to approximately 0.6 ms. These data suggest that the highly mobile residues observed by ^{1}H NMR spectroscopy do not originate from the C-terminus. Binding of Fab directed against the N-terminal amino acids of actin to Mg−F-actin leads to the dissappearing of the ^{1}H NMR resonances assigned to a mobile domain in F-actin. This indicates that the mobile region probably comprises the N-terminal amino acids. By homonuclear two-dimensional ^{1}H NMR spectroscopy it was finally possible to sequentially assign the resonances of the mobile domain of F-actin. It turned out that amino acids 1−22 are in a highly mobile state in Mg−F-actin. The nuclear Overhauser effect data indicate that, rather surprisingly, in this high mobility state some of the β-pleated structure is still conserved. The population of F-actin protomers in the M- (mobile) state can be obtained from the NMR spectra and was determined under different experimental conditions. In the presence of 150 mM KCl approximately half of the protomers in Mg−F-actin are in the M-state. This number is largely independent of the pH in the range studied (pH 7.2−7.8) and of the temperature in range studied (283−310 K). The equilibrium constant K_{MI} for the equilibrium between the I- and M-states is approximately 1.3 under these conditions.

In both its monomeric (G) and its polymerized (F) form actin binds one adenine nucleotide molecule and one divalent metal ion per protomer at a high-affinity binding site. *In vivo* this metal ion is most probably Mg^{2+}, while *in vitro*, as a consequence of the widely used method of actin isolation and purification, it is usually Ca^{2+} (Spudich et al., 1971; Pardee & Spudich, 1982; Estes et al., 1992). In the crystal structure of the actin−DNase I complex (Kabsch et al., 1990), two domains of the protein can be distinguished with the nucleotide−metal complex located in the cleft between these domains. The nature of this complex significantly influences the biochemical and biophysical properties of actin. The type of divalent metal ion as well as the type of the nucleotide bound strongly influences the nucleation and polymerization of actin; the rate of ATP hydrolysis depends on the metal ion present in the active center of actin [for a recent review see Estes et al. (1992) or dos Remedios and Moens (1995)]. However, little is known about structural features of actin that are responsible for these phenomena.

In addition to X-ray crystallography, X-ray fiber diffraction and electron microscopy spectroscopic methods such as NMR can help to elucidate structural differences. A number of NMR studies on actin structure and dynamics in its G- and F-form have been published (Cozzone et al., 1974; Highsmith et al., 1979; Highsmith & Jardetzky, 1980; Barden et al., 1980, 1983, 1989; Barden & dos Remedios, 1984, 1985; Barden & Kemp, 1987; Barden & Philipps, 1990; Prince et al., 1981; Brauer & Sykes, 1981a,b, 1982, 1986; Trayer et al., 1987). Whereas the ^{1}H NMR spectra of G-actin[1] published so far are rather similar, there are large variations between the NMR spectra of F-actin. According to Highsmith and Jardetzky (1979) all resonance lines of F-actin are broadened beyond detection. On the other hand, NMR spectra of F-actin were reported which display intense resonance lines which are very similar to those observed for G-actin (Prince et al., 1981; Trayer et al., 1987). As we could show recently (Slósarek et al., 1994) polymerization of ATP−actin by increasing the ionic strength leads to a quenching of almost all ^{1}H NMR signals. Surprisingly, distinct signals with relatively small line widths can still be observed in actin filaments, indicating the existence of mobile, NMR-visible residues in the macromolecular structure. The intensity of the F-actin spectrum is much reduced if one replaces Mg^{2+} with Ca^{2+}; a weak, not clearly significant reduction of the signal intensity can also be obtained by increasing the ionic strength. These results were

* Author to whom the correspondence should be sent: FAX 06221 486351.

[⊗] Abstract published in *Advance ACS Abstracts,* August 15, 1996.

[1] Abbreviations: DSS, sodium 4,4-dimethyl-4-silapentanesulfonate; G-actin, globular actin; F-actin, filamentous actin; PFP, 4-(perfluoro-*tert*-butyl)phenyliodoacetamide.

S0006-2960(96)01159-2 CCC: $12.00

explained in a two-state model of the actin protomers with an M- (mobile) state and an I- (immobile) state in equilibrium. In the M-state a number of residues in the actin protomer are mobile and give rise to observable NMR signals. This equilibrium is shifted toward the I-state specifically by replacing Mg^{2+} with Ca^{2+} ions. The binding of phalloidin to its high-affinity site in the filaments does not influence the equilibrium between the M- and I-state. Phalloidin itself is completely immobilized in F-actin, its exchange with the solvent being slow on the NMR time scale (Slósarek et al., 1994). Unfortunately, in this study it was not possible to assign the mobile region(s) in Mg−F-actin to a specific part of the structure, information crucial for the biological interpretation of the results.

Studies of F-actin by electron microscopy suggest the existence of various states of F-actin which differ in the overall flexibility of the filaments (Orlova & Egelman, 1992, 1993) and which depend on the type of divalent ions bound to the high (or intermediate) affinity binding site(s). This change of flexibility was associated with a rotation of subdomain 2 and reorientation of the DNase binding loop. High mobility in subdomain 2 encompasing residues 32−52 was also observed in simulations of the G-actin dynamics by normal mode analysis (Tirion & ben-Avraham, 1993). Other plausible candidates for high mobility are the N-and C-termini of the protein and loop 18−29.

In the following we will present the results of ^1H and ^{19}F NMR studies of actin in its G- and F-forms with the aim to define the residues responsible for the high (NMR-visible) mobility in Mg−F-actin.

MATERIALS AND METHODS

Actin Preparation. Actin from rabbit skeletal muscle was prepared from acetone powder as described by Pardee and Spudich (1982) with an additional gel filtration step on a TSK HW 55 (Merck, Darmstadt) (3 × 120 cm) column. The column was equilibrated with either buffer A (2 mM Tris-HCl, 0.2 mM ATP, 0.1 mM $CaCl_2$, 0.002% NaN_3, pH 7.8) or buffer B (2 mM Tris-HCl, 0.2 mM ATP, 0.1 mM $MgCl_2$, 0.2 mM EGTA, 0.002% NaN_3, pH 7.8) to obtain a G-actin with either Ca^{2+} or Mg^{2+} bound at the high-affinity binding site. In order to achieve a highly concentrated F-actin, Mg−G-actin was polymerized in the presence of 30 mM KCl for 30 min at room temperature and subsequently concentrated in a Centriprep-30 concentrator (Amicon) at 4 °C and at 1500*g* to reach a final concentration of 1.2 mM.

Fluorine Labeling of Actin. The fluorine label 4-(perfluoro-*tert*-butyl)phenyliodoacetamide (PFP) was synthesized as described earlier (Kalbitzer et al., 1992). For the selective labeling of Cys-374 3 mg/mL G-actin in buffer A was reacted with a 7-fold excess of PFP diluted in DMF for 18 h at 4 °C. Excess reagent was removed on a Bio-Gel P2 column (1 × 25 cm) equilibrated with buffer A. The exchange of the Ca^{2+} ion with Mg^{2+} at the high-affinity binding site was performed by polymerizing the actin derivative in the presence of 1 mM $MgCl_2$ and 0.4 mM EGTA for 30 min at room temperature. After centrifugation actin was depolymerized in 2 mM Tris, 0.2 mM ATP, 0.1 mM $MgCl_2$, 0.2 mM EGTA, and 0.002% NaN_3, pH 7.8.

Polyclonal Antibodies against the N-Terminal Amino Acids of Actin. Polyclonal antibodies (Fab) against the first seven N-terminal amino acids of actin were obtained as decribed earlier (Miller et al., 1987; DasGupta et al., 1990).

NMR Spectroscopy. One-dimensional ^1H NMR and ^{19}F NMR spectra were recorded on a Bruker AMX-500 NMR spectrometer operating at 500 and 470.4 MHz, respectively. Two-dimensional NMR spectra were measured on a Bruker AMX-600 NMR spectrometer operating at 600 MHz. The water signal was suppressed by selective presaturation. Typically, in one-dimensional NMR spectroscopy 512 free induction decays were accumulated with a repetition time of 5 s including the water suppression pulse of 1 s. Typical acquisition parameters were pulse length 9.4 μs (corresponding to a pulse angle of 80°), spectral width 6024 Hz, delay before acquisition 118.4 μs and 16K data points. Typical processing parameters (used also for the spectra depicted in this paper) were 1 Hz additional line broadening by exponential multiplication of the free induction decay, data size after Fourier transformation 16K, and base-line correction by a third-order polynomial fit. The 600 MHz TOCSY spectrum was recorded with a MLEV16 mixing sequence of 60.4 ms compensated for rotating frame nuclear Overhauser effects according to Kadkhodaei et al. (1993). Water suppression was performed with the WATERGATE sequence (Piotto et al., 1992); 24 free induction decays were accumulated per t_1 increment. The 600 MHz NOESY spectrum was recorded with a mixing time of 150 ms and selective presaturation of the water signal of 1 s. A total of 32 free induction decays were accumulated per t_1 increment; 1024 time domain data points in the t_1 direction and 2024 data points in the t_2 direction were recorded; phase-sensitive detection in the t_1 direction was performed with the TPPI method (Marion & Wüthrich, 1983).

Most of the ^1H NMR spectra were recorded in 5 mm sample tubes; only the 600 MHz spectra were recorded in 8 mm tubes. The outer diameter of the sample tubes used for ^{19}F NMR was 10 mm. Usually, actin was polymerized in the NMR tube by the addition of appropriate aliquots of the stock solutions (3 M KCl, 1 M $MgCl_2$, or 1 M $CaCl_2$). The ^1H NMR spectra are referenced relative to sodium 4,4-dimethyl-4-silapentanesulfonate (DSS) used as internal standard. The G-actin spectrum contains two dominant singlet resonances at 2.048 and 2.066 ppm which do not shift under our experimental conditions. The spectrum of Mg−F-actin contains one singlet resonance at 2.048 ppm (Slósarek et al., 1994). In cases where the addition of DSS was not desirable, these resonances were used for the calibration of the spectra. The ^{19}F NMR spectra were referenced to trifluoracetic acid contained in a small glass sphere (Wilmad) immersed in the sample. Where not indicated otherwise, the measurements were performed at 278 K.

Analysis of the NMR Data. The NMR data were filtered and phase-corrected with the program UXNMR (Bruker, Karlsruhe). Further steps in the data evaluation were performed with the program AURELIA (Neidig et al., 1995). Base-line corrections in the two-dimensional spectra were performed according to Saffrich et al. (1993); peak integration was performed with an optimized iterative segmentation procedure (Geyer et al., 1995) using a segmentation threshold of 5% of the peak maximum.

The relative integrals of the *N*-acetyl peak in the one-dimensional spectra of G- and F-actin were determined with three different methods: (1) numerical integration of the peak area after removing all broad background signals except the sharp methyl signals by a spline interpolation, (2) fitting the lines by Lorentzians, and (3) after adjusting for the differences in line widths in the G- and F-actin spectra (which

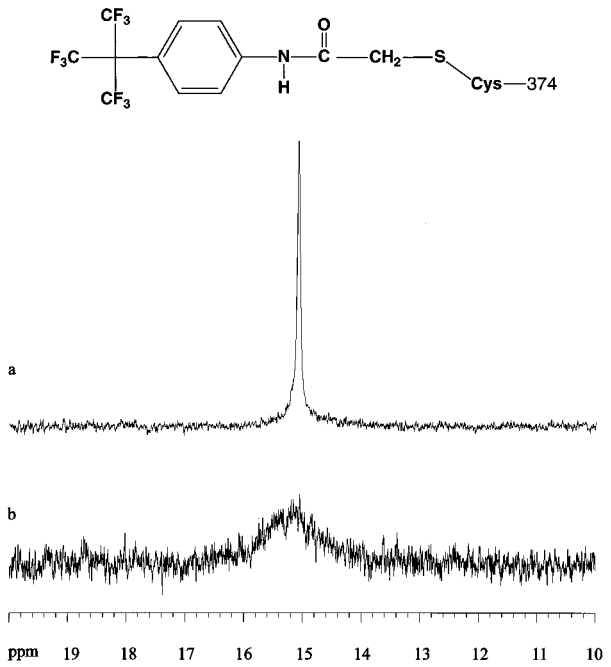

FIGURE 1: ^{19}F NMR spectra of fluorine-labeled G-actin and F-actin. (Top) Structure of the fluorine label PFP bound to Cys-374 of actin. (Midldle) ^{19}F NMR spectrum of PFP-labeled Mg−G-actin. (Bottom) ^{19}F NMR spectrum of PFP-labeled Mg−F-actin. The Mg−G-actin sample contained 74 μM Mg−actin labeled with PFP at Cys-374 in 0.2 mM ATP, 0.1 mM $MgCl_2$, 0.2 mM EGTA, 2 mM Tris-HCl, 0.002% NaN_3, pH 7.7, and 90% H_2O/10% D_2O. After the G-actin spectra were recorded, the protein was polymerized in the NMR tube by the addition of 5 μL of a 3 M KCl solution (end concentration 30 mM). The spectra were recorded at 283 K; the experimental conditions (except the number of scans) and the data processing were identical for the two spectra.

can be done by a suitable exponential multiplication) interactive determination of the scaling factor which leads to identical signals in the two spectra. The interactive method was performed in the dual display mode of the program UXNMR and was shown to be most reliable and most reproducible. However, all three methods gave comparable values. The relative integrals reported below were obtained by method 3.

RESULTS

PFP-Labeled G- and F-Actin. We had observed earlier that after polymerization of Mg^{2+}−actin in the ^{1}H NMR spectra the signals of a number of mobile residues remained visible. Characteristically, these signals were not visible in Ca^{2+}−F-actin and were quenched in Mg^{2+}−F-actin with increasing KCl concentration (Slózarek et al., 1994). The important question, which part of the molecule remains flexible after polymerization, has not been answered yet. A plausible location would be the C-terminus which is accessable for proteases; its removal influences the ATPase activity and the polymerization rate (Strzelecka-Golaszewska, 1995). The C-terminal sequence of actin contains a cysteine residue (Cys-374) whose sulfhydryl group can be easily modified. Labeling of this group with the high-sensitivity fluorine label PFP (Kalbitzer et al., 1992) should allow the monitoring of the internal mobility in this part of the structure by ^{19}F NMR. Figure 1 shows the results for Mg−actin: The spectrum of labeled Mg−G-actin exhibits the expected rather narrow signal at 15.06 ± 0.03 ppm, which is substantially broadened after polymerization with KCl. This is different to the effect observed in the ^{1}H NMR spectra where rather sharp lines are still visible after polymerization and suggests that the fluorine label is not located in the mobile, NMR-visible region. The full line width at half-height $\Delta\nu_{1/2}$ is 19 Hz for Mg−G-actin, corresponding to a transverse relaxation time of 16.7 ms at 283 K. After polymerization the line width $\Delta\nu_{1/2}$ is 520 ± 40 Hz in the spectrum shown, corresponding to a transverse relaxation time of 0.6 ms. This line width varies somewhat from preparation to preparation probably due to differences in the viscosity of the solution. The peak maximum seems to shift downfield after polymerization (an effect which is very difficult to substantiate because of the large line width). Analogous results are obtained for Ca−actin; again the sharp line of Ca−G-actin broadens after polymerization (data not shown). In the limits of error identical line positions and line widths in free and polymerized actin seem to be independent of the ion in the active center.

^{1}H NMR Spectra of F-Actin−Fab Complexes. A different approach to assign the ^{1}H NMR visible resonances is the immobilization of the corresponding residues by specific antibodies. Since Fabs against the seven N-terminal amino acids are available, the hypothesis that at least part of the observable resonances originate from the N-terminus was tested experimentally. Addition of this antibody to Mg−F-actin leads to the attenuation and finally to the disappearance of some signals which are typical for Mg−F-actin. The most clearly detectable resonance is the already described singlet resonance at 2.048 ppm (labeled as N-ACE in Figure 2) which must be due to a methyl group of the N-terminal acetyl or a methionine residue (Slósarek et al., 1994). Since this signal disappears, it comes most probably from the *N*-acetyl group (Figure 2). (However, there is a slight chance that the observed effect is an unspecific long-range effect. This is excluded by the direct NMR sequencing discussed below.) Somewhat disappointingly after saturation of F-actin with the antibody there are still some signals observable. This could mean that part of the signal of Mg−F-actin is not quenched by the antibody binding. However, a closer inspection of the data shows that the spectrum of the complex is different from that of free Mg−F-actin, suggesting that at least part of the signals originate from mobile regions in the antibody itself. A simple possibility to test this assumption is the already described immobilization of the residues visible in Mg−F-actin by the addition of calcium ions (Figure 3). At least in a first approximation the actin resonances should also be quenched in the complex and the remaining lines should be due to the bound antibody. Figure 3 demonstrates that the bound antibody has mobile residues which are visible in the complex.

Two-Dimensional NMR Spectroscopy of Mg−F-Actin. The basis for the well-developed NMR structure determination of small proteins is the ability to sequentially assign resonances by multidimensional methods. These methods should also be applicable to the mobile regions in Mg−F-actin. At the low concentrations in the submillimolar range usually available for actin, the signal-to-noise ratio is not sufficient for such an assignment. However, after concentrating the F-actin solution by more than a factor of 30, spectra with sufficient quality could be obtained. Figure 4 shows the complete TOCSY spectrum of a 1.2 mM solution

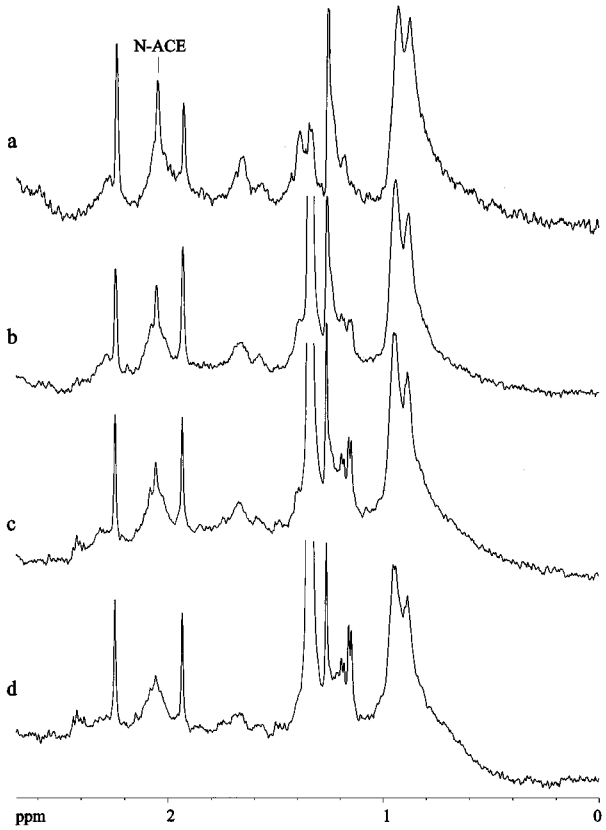

FIGURE 2: ^{1}H NMR spectra of the Mg−F-actin complex with Fab. Part of the 500 MHz ^{1}H NMR spectra of Mg−actin complexed with Fabs against the first seven N-terminal amino acids of actin. The sample contained 27 μM Mg−actin in 30 mM KCl, 0.2 mM ATP, 0.1 mM $MgCl_2$, 0.2 mM EGTA, 2 mM Tris-HCl, pH 7.8, 90% H_2O/10% D_2O, and various quantities of Fab. The molar ratio of Fab/actin was varied between 0 (a), 0.27 (b), 0.7 (c), and 1 (d). Temperature was 283 K; identical parameters were used for recording, processing, and representation of the spectra. Noise reduction was by exponential multiplication corresponding to an additional line broadening of 3 Hz.

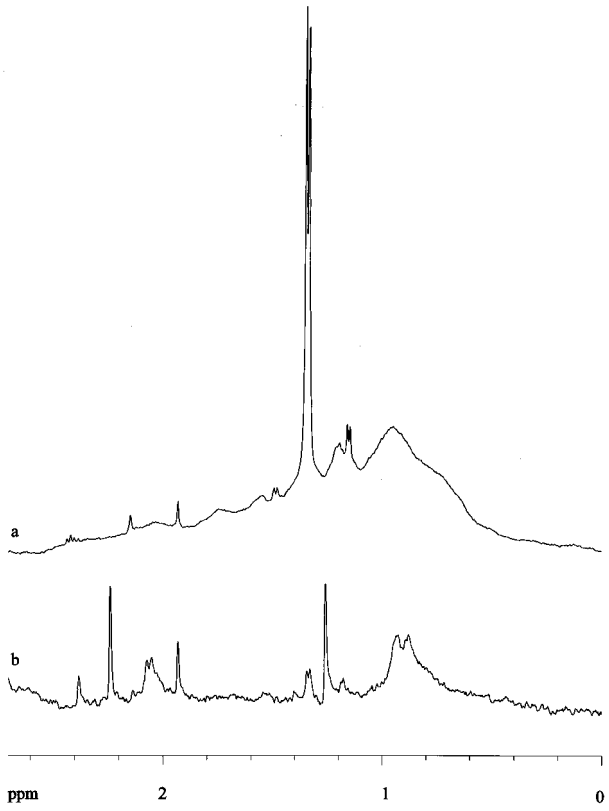

FIGURE 3: ^{1}H NMR spectra of free Fab and Fab bound to Ca−F-actin. Part of the 500 MHz ^{1}H NMR spectra of free Fab against the N-terminus of actin (a) and of the actin-bound Fab (b). Sample a contained 72 μM Fab in 30 mM KCl, 2 mM Tris-HCl, pH 7.8, and 90% H_2O/10% D_2O; sample b contained 26.8 μM Mg−actin and 14.3 μM Fab in 30 mM KCl, 0.13 mM ATP, 0.06 mM $MgCl_2$, 5 mM $CaCl_2$, 0.13 mM EGTA, 2 mM Tris-HCl, pH 7.8, and 90% H_2O/10% D_2O. The temperature was 283 K; identical parameters were used for recording, processing, and representation of the spectra. Noise reduction was by exponential multiplication corresponding to an additional line broadening of 3 Hz.

of Mg−F-actin which shows a number of cross peaks as they would be typical for a small peptide of approximately 20 amino acids. Together with DQF-COSY spectra and NOESY spectra it was possible to obtain the sequential assignments of the resonances (Table 1). Figure 5 shows the amide−Hα fingerprint region of the TOCSY spectrum with the peak assignments. A good starting point for the sequential assignment is the singlet resonance at 2.05 ppm which, in principle, could originate from either a methyl group of a methionine residue or the N-terminal acetyl moiety. Since there is a strong NOE cross peak to the amide resonance of an Asx residue, the NMR data indicate strongly the assignment of this signal to the N-terminal acetyl group. This agrees perfectly with the independent evidence derived from the antibody experiments presented above. The sequential assignment of the first 15 amino acids was straightforward since sequential NOEs exist (Figure 6) and the characteristic spin systems could be completely found in the TOCSY spectra (Figure 4). The side chain amide resonances could be linked to the rest of the Asn spin system via their NOE to the Hβ of the side chain. Only the resonance position of the second Hβ of Asn-12 and the second Hα of Gly-15 could not be assigned unambiguously. For Leu-16 a separate spin system with cross peaks differing from those of Leu-8 could not be identified. However, integration of the methyl region in one-dimensional spectra suggests that at least an additional pair of leucyl methyl

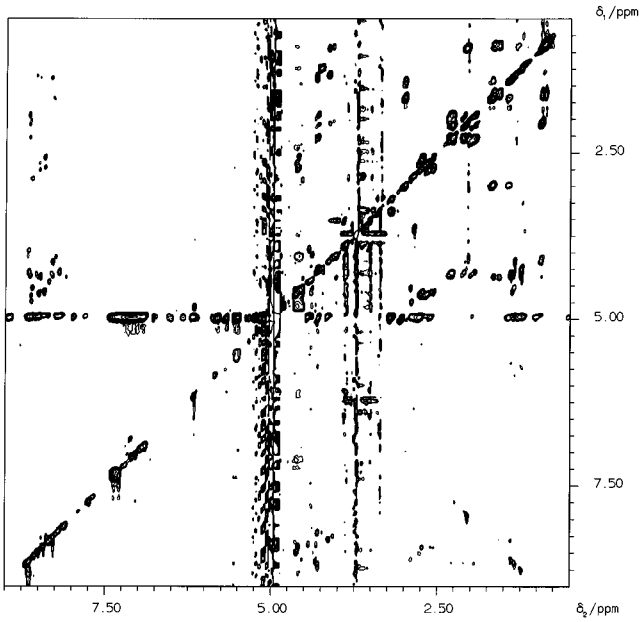

FIGURE 4: TOCSY spectrum of Mg−F-actin. 600 MHz ^{1}H NMR spectrum of 1.2 mM Mg−F-actin, 30 mM KCl, 0.1 mM $MgCl_2$, and 0.2 mM EGTA in 2 mM Tris-HCl, pH 7.8. The data were recorded at 289 K with an isotropic mixing time t_m of 60.4 ms.

resonances must be present to explain the experimental data. Most probably the spin system of Leu-16 overlaps strongly with that of Leu-8. The next three amino acids in the

Table 1: Mobile Residues in Mg−F-Actin[a]

	chemical shift (ppm) relative to DSS						
residue	H	Hα	Hβ	Hγ	Hδ	Hϵ	Hζ
N-ACE			2.05				
Asp-1	8.41	4.58	2.57, 2.73				
Glu-2	8.64	4.29	1.93, 2.10	2.26, 2.30			
Asp-3	8.49	4.61	2.65, 2.75				
Glu-4	8.62	4.33	1.99, 2.12	2.27, 2.33			
Thr-5	8.47	4.36	4.26	1.24			
Thr-6	8.18	4.29	4.22	1.23			
Ala-7	8.31	4.31	1.38				
Leu-8	8.28	4.35	1.56, 1.67	1.64	0.88, 0.94		
Val-9	8.28	4.14	2.07	0.94, 0.96			
Cys-10	8.62	4.65	2.68, 2.74				
Asp-11	8.59	4.52	2.89, 2.89				
Asn-12	8.61	4.73	2.88	3.21[b]	7.04	7.73	
Gly-13	8.65	3.96, 4.43					
Ser-14	8.34	4.43	3.89, 3.93				
Gly-15	8.08	4.36					
Leu-16	−[c]						
Val-17	8.25	4.07	2.03	0.92, 0.95			
Lys-18	8.54	4.30	1.68, 1.82	1.41, 1.45	1.66, 1.68	2.98	
Ala-19	8.54	4.35	1.36				
Gly-20	−[c]						
Phe-21	−[c]	4.63	3.05, 3.17		7.28, 7.28	7.36, 7.36	7.32
Ala-22	8.48	4.36	1.38				

[a] Experimental conditions as described in Figure 4. [b] Cross peaks very weak, spin system can be assigned only tentatively. [c] Not identified.

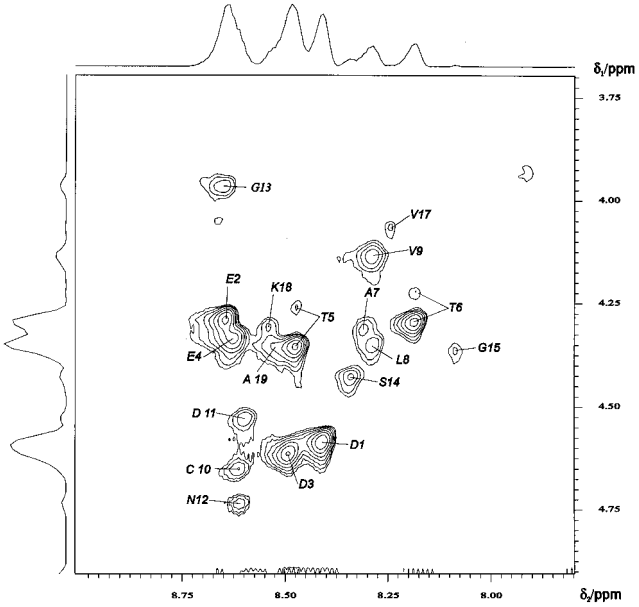

FIGURE 5: Amide−Hα region of a TOCSY spectrum of Mg−F-actin. Shown is part of the TOCSY spectrum depicted in Figure 4 but with the assignments of the cross peaks indicated.

sequence could be identified without problem in the two-dimensional NMR spectra. Distinct amide−Hα cross peaks were not observable for Gly-20 and Phe-21 although it could be possible that they are existing but superposed by amide−Hα cross peaks of other amino acids. The Hδ of the aromatic ring of Phe-21 shows the expected NOE cross peaks to the β-protons of its side chain. An additional NOE to the Hα completes this assignment.

Structure and Dynamics of the N-Terminal Part of Mg−F-Actin. Since the nuclear Overhauser effect as basis for the structural determination depends on the correlation times τ and on the motional modes described by the correlation function f(τ), it appears quite unreasonable to try to quantify these effects in such a complicated system as F-actin. However, with a few assumptions one can get at least to semiquantitative results.

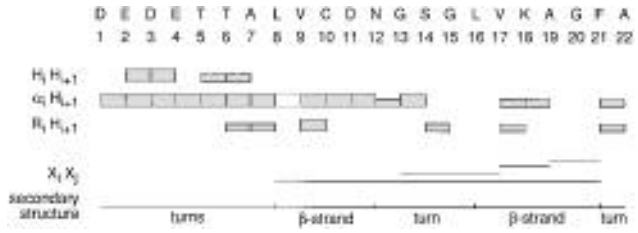

FIGURE 6: Sequential and long-range NOEs. Plot of the NOE intensities in the ^{1}H NMR spectrum for amino acids i and j: H_iH_{i+1}, NOE between amide protons of amino acids i and i+1; α_iH_{i+1}, NOE between the Hα and the amide proton; and R_iH_{i+1}, NOE between a side chain proton and the amide proton; X_i X_j, NOE between main chain or side chain protons of two amino acids i and j with $j > i$+1. The strong α_i H_{i+1} NOE between amino acids 8 and 9 (indicated by broken lines) most probably exists but is superposed by the internal α_iH_i NOE of amino acid 8. The secondary structure elements were taken from the crystal structure of actin (Kabsch et al., 1990).

Since only negative NOEs are observed (NOE cross peaks with the same sign as the diagonal signals), the relevant apparent correlation time τ_a must fulfill the condition $2\pi\nu_0\tau_a > 5^{1/2}/2$. From the resonance frequency ν_0 of 600 MHz one obtains a τ_a that must be larger than 0.3 ns. For short mixing times t_m the cross peak intensities V_{ij} in the TOCSY spectrum can be approximated by $A \sin^2(\pi J_{ij} t_m)\ e^{-t_m/T_{1\rho}}$ with A a constant, J_{ij} the J coupling between spin i and spin j, and $T_{1\rho}$ the longitudinal relaxation rate in the rotating frame of spin i induced by spin j. Under the (not completely true) assumption that the coupling constants J_{ij} are equal (sufficiently similar), ln V_{ij} is linearily dependent on $t_m/T_{1\rho}$ and hence on the apparent τ_a. The plot of ln V_{ij} of the Hα−amide cross peaks of residues i and i + 1 as in dependence of residue number i is shown in Figure 7. If one considers the cross peak volumes, three groups can be distinguished, a group with relatively high volumes (Asp-1 to Thr-6), a group with significantly lower volumes (Ala-7 to Ser-14), and a group with variable but small volumes starting with Gly-15. For Leu-16, Gly-20, and Phe-21 Hα−amide cross peaks could not be observed unequivocally; the cross peak of Ala-22 is located in a crowded region where no precise

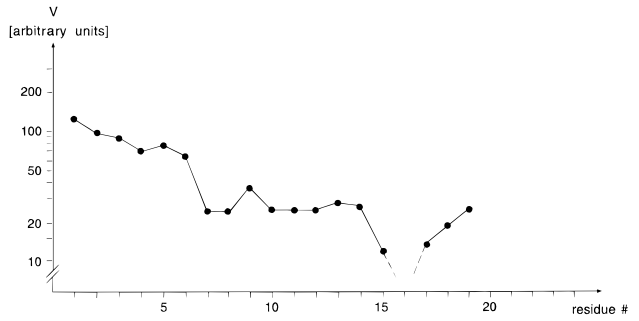

FIGURE 7: Cross peak intensities in the mobile region of actin. Logarithmic plot of the TOCSY cross peak volumes with respect to dependence of the residue number.

NOE could be determined. However, since the whole spin system of Leu-16 could not be identified, it is very likely that also the Hα−amide cross peak is very weak. The other Hα−amide cross peak may be superposed by more intense cross peaks of other residues. In the first group ln V_{ij} varies between 4.2 and 4.8 and in the second group between 3.2 and 3.3 (if one neglects the rather strong signal of Val-9). The lowest value is obtained with 2.5 for Gly-15.

Besides the sequential NOEs some intermediate-range and long-range NOEs could be observed (Figure 6). Of particular interest is the long-range NOE between the Hδ protons of Leu-8 and the ring protons of Phe-21 (Hδ and Hϵ), since they indicate that these two amino acids are at least in the time average in contact in solution as is true for the crystal structure. Another important long-range NOE can be observed between the amide proton of Gly-13 and the Hα of Val-17; it is again indicative for a contact between the two β-strands in solution. If the first β-pleated sheet described in the crystal structure should also exist in the mobile state of F-actin, Hα−Hα NOEs between the amino acids of the two strands should be observable. From our data their existence could not be verified unambiguously, mainly because of the limited quality of the data in this part of the spectrum.

Influence of pH and Temperature on the Mobile Domain of F-Actin. An important question is under which conditions, the mobilty in the protomers of F-actin remains preserved since low ionic strength, 283 K, and pH 7.8 are not physiological. Therefore, the intensity dependence of the NMR signals was studied as a function of these parameters. The biologically important value is the number of protomers in the M-state and the I-state in the filament or the equilibrium constant between the two states. This can be done by integration of the resonance lines. Since base-line artifacts on the integrals are very difficult to avoid if broad and weak NMR signals are selected, it is better to select a representative, well-resolved signal for the integration. Figure 8 shows the spectral range where the signal of the *N*-acetyl group can be observed. In the G-actin spectrum a second sharp resonance can be observed besides the signal at 2.048 from the *N*-acetyl group which disappears after polymerization. It can be assigned to the methyl groups of two methionine residues. In the absence of further experimental evidence one may speculate on their origin. Possible candidates for methionine residues which are located in a highly flexible region in G-actin and in a rigid region in F-actin would be Met-44 and Met-47. They are part of the DNase binding loop which is supposed to be flexible in G-actin but probably mediates contacts between the protomers in F-actin. The integrals of the *N*-acetyl signals in

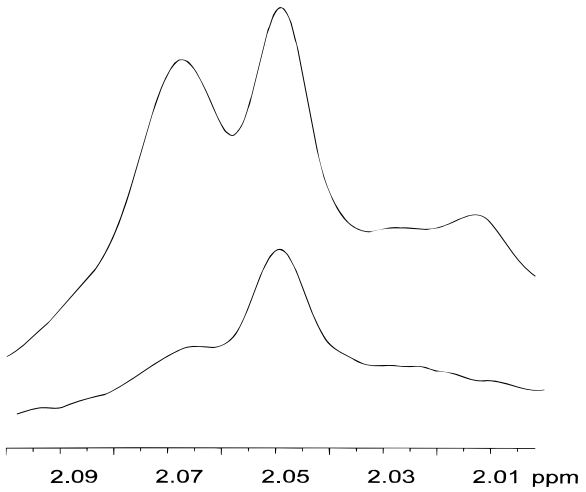

FIGURE 8: *N*-Acetyl signal in G- and F-actin. ^{1}H NMR spectrum from Mg−actin at pH 7.8 and 298 K before (upper trace) and after polymerization with 30 mM KCl.

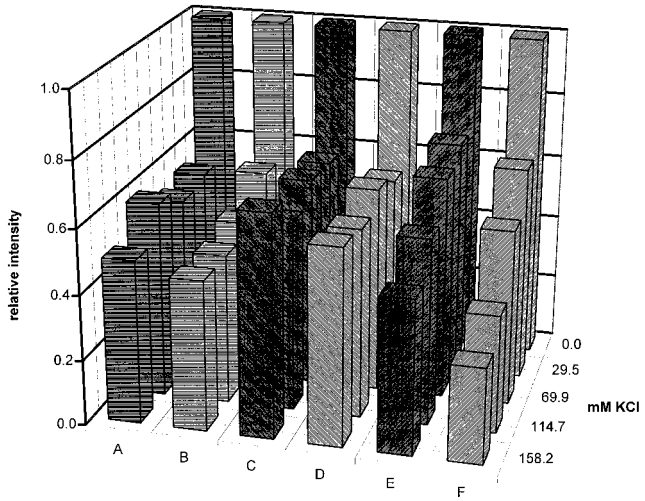

FIGURE 9: Population of the M- and I-states in Mg−F-actin. The sample contained 0.05 mM Mg−actin in 0.2 mM ATP, 0.1 mM $MgCl_2$, 0.2 mM EGTA, 2 mM Tris-HCl, and 90% H_2O/10% D_2O with KCl in various concentrations. The pH and temperature were varied in different experiments: (A) pH 7.8, 283 K; (B) pH 7.2, 283 K; (C) pH 7.8, 298 K; (D) pH 7.2, 298 K; (E) pH 7.8, 310 K; (F) pH 7.2, 310 K.

F-actin were determined under different experimental conditions and normalized to the *N*-acetyl signal of G-actin of the same sample. The relative integrals of the *N*-acetyl signal in G- and F-actins were determined as described in Materials and Methods. They are plotted in Figure 9. As to be expected the relative signal intensities vary from spectrum to spectrum (probably due to integration errors), but under all conditions a substantial part of the actin protomers remains in the M-state. The rather large experimental error does not allow us to decide if in the ionic strength range studied here the intensity depends on the ionic strength as suggested earlier for a larger range (Slósarek et al., 1994). The mean value of all measurements is 0.56 with a standard error of 0.1; that is, under the assumption that the total error is only due to statistical errors, the equilibrium constant $K_{MI} = [A_M]/[[A_I]$ for the equilibrium between protomers A_M and A_I in the M- and I-state is 1.3.

DISCUSSION

Structural Aspects. As we have shown earlier F-actin preparations polymerized from Mg−G-actin in the presence

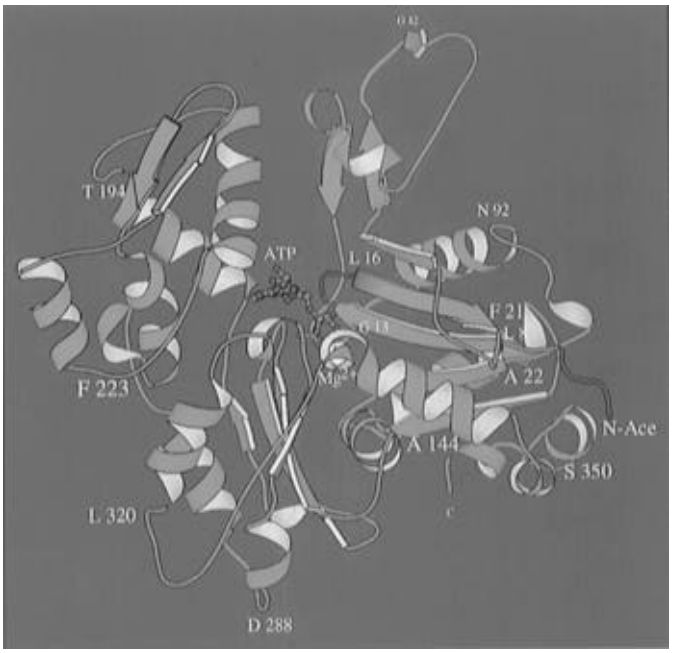

FIGURE 10: Mobile amino acids in Mg−F-actin. The NMR-visible residues in Mg−F-actin are shown in the X-ray structure of Ca−F-actin from Kabsch et al. (1990). The color code corresponds to differences in internal mobility with red indicating the highest mobility and blue the lowest mobility.

of ATP but not from Ca−G-actin show still clearly defined ^{1}H NMR signals. All biochemical and NMR evidence indicated that these signals originated from mobile segments in F-actin and were not due to impurities in the sample (Slósarek et al., 1994). Our NMR experiments presented here show that in Mg−F-actin approximately half of the protomers are in the M-state, a state with high internal mobility. The mobile region could be unequivocally identified to be located in the N-terminal region of the protein comprising the N-terminus itself and the first two strands of the large N-terminal β-pleated sheet (Figure 10). The sequential assignments prove that the observed signals cannot come from a protein impurity but have to come from actin itself. The quantification of the signals (and their independence on details of the actin purification procedure) makes it extremely unlikely that these signals originate from denatured actin, since it would mean that half of our protein and of the protein prepared by all other groups in the actomyosin field with the standard purification procedure (Spudich et al., 1971) would be denatured. The intensities of the TOCSY cross peaks (Figure 7) and the line widths in one-dimensional spectra indicate that the first six N-terminal amino acids exhibit the highest mobility and the two antiparallel strands an intermediate mobility with the lowest mobility in the β-turn region. An initial inspection of the apparently well-ordered and densily packed structure suggests that in Mg−F-actin this part of the structure must be changed dramatically. A possible explanation would be an almost complete unfolding of this region accompanied by an increase of the local mobility in the polypeptide main chain. In line with this suggestion would be structural studies on the N-terminal peptide (28 amino acids) of actin by Sönnichsen et al. (1992). In aqueous solution the peptide was not ordered and very flexible; in 80% trifluoroethanol they found two helices from residues 4 to 13 and 16 to 20 with a β-turn formed by residues 13−16. No long-range NOEs between the two helices were observed. The data indicate that the β-pleated structure of this region in actin is mainly stabilized by the protein environment; only a propensity for the formation of the β-turn observed in native actin seems to exist in the isolated peptide. However, our NOE pattern indicates that in our case the β-pleated structure and the contacts between the two strands remain essentially intact. The chemical shifts of corresponding resonances observed by us in F-actin and by Sönnichsen et al. (1992) in the free peptide in the presence of trifluoroethanol are very different, indicating again that the mobile part in F-actin has a structure which differs completely from the peptide structure induced by trifluoroethanol. Chemical shift values in the absence of trifluoroethanol were not reported in detail by Sönnichsen et al. (1992), but they claimed to find only chemical shift values typical for random-coil peptides. The NOE pattern observed by us in F-actin (Figure 6) strongly suggests that the two N-terminal strands still form a β-pleated sheet. Consequently, a number of chemical shift values given in Table 1 differ significantly from the typical random-coil values (Bundi & Wüthrich, 1979; Wishart et al., 1992).

A closer inspection of the X-ray structure of G-actin of Kabsch et al. (1990) reveals that the β-pleated sheet containing the two N-terminal, mobile strands is rather distorted. The analysis of the published coordinates with the program DSSP (Kabsch & Sander, 1990) indicates that nevertheless the β-pleated sheet seems to be well stabilized by hydrogen bonds with rather favorable electrostatic energies. The two strands, 8−14 and 16−21, are stabilized internally by the hydrogen bonds (9 NH → 20 O, 9 O ← 20 NH, 11 NH → 18 O, 11 O ← 18 NH, 13 NH → 16 O). They are fixed to the antiparallel strand 28−33 by five additional bonds (15 O ← 33 NH, 17 NH → 31 O, 17 O ← 31, 19 NH → 29 O, 19 O ← 29 NH) and to the parallel strand by four hydrogen bonds (8 NH → 102 O, 8 O ← 104 NH, 10 NH → 104 O, 10 O ← 106 NH). Only three of these bonds (9 O ← 20 NH, 13 NH → 16 O, 10 O ← 106 NH) are with electrostatic energies above −3.6 kJ/mol rather weak. In addition, the high-affinity Ca^{2+} ion is coordinated to one of the Oδ's of Asp-11 in the ADP complex and to Oδ1 and Oδ2 of Asp-11 in the ATP complex (note that as in most other studies of so-called ATP−F-actin, probably an ill-defined mixture of di- and triphosphates is present in the filaments). The phosphate moieties of the nucleotide also help to fix the strand which is mobile in Mg−F-actin in Ca−G-actin: In the ADP complex hydrogen bonds between the oxygens of the β-phosphate group and the amide groups of Ser 14, Gly-15, and Leu-16 exit; in the ATP complex an additional bond could exist to an oxygen of the γ-phosphate group and the amide proton of Ser-14.

It is very difficult to imagine that this network of interactions should allow a fast movement of the two β-strands in G-actin, especially since this region is one of the regions with the lowest temperature factors in the crystal structure. This means that in Mg−F-actin the conformational state of the actin protomers (or more precise, of half of the protomers) must differ at some point from the crystal structure of Ca−G-actin. As stated above, the NOE patterns observed strongly indicate that the β-pleated stucture of the two N-terminal strands is still conserved in Mg−F-actin. A plausible structural model would state that the replacement of Ca^{2+} by Mg^{2+} in actin may weaken the interaction of amino acid 11 with the metal ion together with a weakening of the hydrogen bonds to the neighboring strands by the actin−actin interactions after polymerization. In line with this notion are the observations by Adams and Reisler

(1994): They observed that the metal ion at the high-affinity cation binding site influences the binding of antibodies against amino acids 18−29 to F-actin; that is, the conformation of this part of the structure (which is just in contact with our high-mobility site) changes when Ca^{2+} is replaced by Mg^{2+}.

In the literature a number of other regions of high flexibility in F-actin are suggested (see the introduction). The question arises if the NMR data exclude their existence. Since the NMR spectrum of F-actin is completely assigned, the NMR data exclude that under our experimental conditions other regions in actin exist which show the same high mobility (corresponding to a rather similar large transverse relaxation time) as observed for the N-terminus and represent an appreciable population of F-actin protomers. Especially the C-terminus which has been assumed to be highly mobile seems to be not very mobile in F-actin as the ^{1}H and the ^{19}F NMR experiments show. However, this is only true in the NMR time scale of our experiments (nanoseconds). Slower movements or movements with small amplitude would not be visible in our experiments and could therefore exist in other regions of the molecule.

A more detailed analysis of the internal motions could be done by relaxation measurements and H/D exchange experiments on isotope-enriched actin. Unfortunately, no bacterial expression system for skeletal muscle actin is known which produces larger quantities of natively folded protein.

Functional Meaning of the High Mobility. According to our results approximately half of the protomers in Mg−F-actin are in the M-state with the N-terminal amino acids in a highly mobile state. The first six amino acids are not in close contact with the rest of the protein but probably stick out into the solution. Since the N-terminal amino acids are assumed to be one of the primary contact sites to myosin-S1, such a picture would make sense since the free ends of actin could be fishing for the myosin heads in their environment. Assuming that the number of protomers in the M-state is similar in the intact muscle (which is not a trivial assumption), the equilibrium between these two states could have some function in the regulation of the interaction of myosin heads with actin filaments; e.g., if they should be notrandomly distributed on the filament, they could help to regulate the separation of myosin interaction sites on F-actin. Such a cooperativity could be induced by thermal movements in the filaments: undulative motions in solution (as they are also observed in the in vitro motility assays) would lead to mutual compressive and tensile forces on the protomers depending on the actual position of the protomers in the filaments. Small but long-range distortions of the linear filament structure could even be imagined in intact muscle fibers, especially after interaction with myosin heads during the force development.

ACKNOWLEDGMENT

We are grateful to K. C. Holmes for his continuous support and many helpful discussions and to E. Reisler for providing the antibodies against the N-terminal residues of actin and for a critical discussion of the results. We thank H. Oschkinat for giving us access to the 600 MHz spectrometer of the EMBL and L. Mitschang for help with this spectrometer.

REFERENCES

Adams, S. B., & Reisler, E. (1994) *Biochemistry 33*, 14426−14433.

Akasaka, K., Ishima, R., & Shibata, S. (1990) *Phys. B 164*, 163−179.

Barden, J. A., & dos Remedios, C. G. (1984) *J. Biochem. 96*, 913−921.

Barden, J. A., & dos Remedios, C. G. (1985) *Eur. J. Biochem. 146*, 5−8.

Barden, J. A., & Kemp, B. E. (1987) *Biochemistry 26*, 1471−1478.

Barden, J. A., & Phillips, L. (1990) *Biochemistry 29*, 1348−1354.

Barden, J. A., Cooke, R., Wright, P. E., & dos Remedios, C. G. (1980) *Biochemistry 19*, 5912−5916.

Barden, J. A., Wu, C.-S., & dos Remedios, C.*G*. (1983) *BBA 748*, 230−235.

Barden, J. A., Phillips, L., Cornell, B. A., & dos Remedios, C. G. (1989) *Biochemistry 28*, 5895−5901.

Brauer, M., & Sykes, B. D. (1981a) *Biochemistry 20*, 2060−2064.

Brauer, M., & Sykes, B. D. (1981b) *Biochemistry 20*, 6767−6775.

Brauer, M., & Sykes, B. D. (1982) *Biochemistry 21*, 5934−5939.

Brauer, M., & Sykes, B. D. (1986) *Biochemistry 25*, 2187−2191.

Bundi, A., & Wüthrich, K. (1979) *Biopolymers 18*, 285−297.

Cozzone P. J., Nelson D. J., & Jardetzky O. (1974) *Biochem. Biophys. Res. Commun. 60*, 341−347.

DasGupta, G., White, J., Philips, M., Bulinski, J. C., & Reisler, E. (1990) *Biochemistry 29*, 3119−3324.

dos Remedios, C. G., & Moens, P. D. J. (1995) *Biochim. Biophys. Acta 1228*, 99−124.

Estes, J. E., Selden, L. A., Kinosian, H. J., & Gershman, L. C. (1992) *J. Muscle Res. Cell Motil. 13*, 272−284.

Geyer, M., Neidig, K.-P., & Kalbitzer, H. R. (1993) *J. Magn. Reson. B109*, 31−38.

Highsmith, S., & Jardetzky, O. (1980) *FEBS Lett. 121*, 55−60.

Highsmith, S., Akasaka, K., Konrad, M., Goody, R., Holmes, K., Wade-Jardetzky, N., & Jardetzky, O. (1979) *Biochemistry 18*, 4238−4244.

Kabsch, W., Mannherz, H. G., Suck, D., Pai, E. F., & Holmes, K. C. (1990) *Nature 347*, 37−44.

Kadhodaei, M., Hwang, R.-L., & Shaka, A. J. (1993) *J. Magn. Reson. A105*, 104−107.

Kalbitzer, H. R., Rohr, G., Nowak, E., Goody, R. S., Kuhn, W., & Zimmermann, H. (1992) *NMR Biomed. 5*, 347−350.

Marion, D., & Wüthrich, K. (1993) *Biochem. Biophys. Res. Commun. 112*, 967−974.

Miller, L., Kalnoski, M., Yunossi, Z., Bulinski, J. C., & Reisler, E. (1987) *Biochemistry 26*, 6064−6070.

Neidig, K.-P., Geyer, M., Görler, A., Antz, C., Saffrich, R., Beneicke, W., & Kalbitzer, H. R. (1995) *J. Biomol. NMR 6*, 255−270.

Orlova, A., & Egelman, E. H. (1992) *J. Mol. Biol. 227*, 1043−1053.

Orlova, A.., & Egelman, E. H. (1993) *J. Mol. Biol. 232*, 334−341.

Pardee J., & Spudich J. S. (1982) *Methods Enzymol. 89*, 164−181.

Phillips, L., Separovic, F., Cornell, B. A., Barden, J. A., & dos Remedios, C. G. (1991) *Eur. Biophys. J. 19*, 147−155.

Piotto, M., Saudek, V., & Sklenar, V. (1992) *J. Biomol. NMR 2*, 661−665.

Prince, H. P., Trayer, H. R., Henry, G. D., Trayer, I. P., Dalgarno, D. C., Levine, B. A., Cary, P. D., & Turner, Ch. (1981) *Eur. J. Biochem. 121*, 213−219.

Saffrich, R., Beneicke, W., Neidig, K.-P., & Kalbitzer, H. R. (1993) *J. Magn. Reson. B101*, 304−308.

Slósarek, G., Heintz, D., & Kalbitzer, H. R. (1994) *FEBS Lett. 351*, 405−410.

Sönnichsen, F. D., van Eyck, J. E., Hodges, R. S., & Sykes, B. D. (1992) *Biochemistry 31*, 8790−8798.

Spudich, J. A., & Watt, S. (1971) *J. Biol. Chem. 256*, 4866−4876.

Strzelecka-Golaszewska, H., Mossakowska, M., Wozniak, A., Moraczevska, J., & Nakayama, H. (1995) *Biochem. J. 307*, 527−534.

Tirion, M. M., & ben-Avraham, D. (1993) *J. Mol. Biol. 230*, 186−195.

Trayer, I. P., Trayer, H. R., & Levine, B. A. (1987) *Eur. J. Biochem. 164*, 259−266.

Wishart, D. S., Sykes, B. D., & Richards, F. M. (1992) *Biochemistry 31*, 1674−1651.

BI961159K